

Field-theoretic description of ionic crystallization in the restricted primitive model

A. Ciach¹ and O. Patsahan²

¹*Institute of Physical Chemistry, Polish Academy of Sciences, 01-224 Warszawa, Poland*

²*Institute for Condensed Matter Physics of the National Academy of Sciences of Ukraine, 1 Svientsitskii Strasse, 79011 Lviv, Ukraine*

(Received 25 April 2006; published 23 August 2006)

Effects of charge-density fluctuations on a phase behavior of the restricted primitive model are studied within a field-theoretic formalism. We focus on a λ line of continuous transitions between charge-ordered and charge-disordered phases that is observed in several mean-field theories, but is absent in simulation results. In our study the RPM is reduced to a ϕ^6 theory, and a fluctuation contribution to a grand thermodynamic potential is obtained by generalizing the Brazovskii approach. We find that in a presence of fluctuations the λ -line disappears. Instead, a fluctuation-induced first-order transition to a charge-ordered phase appears in the same region of a phase diagram, where the liquid–ionic-crystal transition is obtained in simulations. Our results indicate that the charge-ordered phase should be identified with an ionic crystal.

DOI: [10.1103/PhysRevE.74.021508](https://doi.org/10.1103/PhysRevE.74.021508)

PACS number(s): 61.20.Qg, 64.10.+h, 64.60.Cn

I. INTRODUCTION

Molten salts, ionic liquids or electrolytes can be described by the restricted primitive model (RPM), where impenetrable hard cores of diameter σ carry charges with equal magnitude e [1,2]. In the continuum-space RPM a separation into uniform ion-dilute and ion-dense phases with an associated critical point occurs at low densities, a transition to an ionic crystal of the CsCl type occurs at intermediate densities, and at high densities the fcc crystal is stable [3]. The above phase-behavior was confirmed by simulations [4–6]. The fcc crystal undergoes a weakly first-order transition between a high-temperature phase without a substitutional order and a low-temperature phase of the tetragonal [4,6] symmetry. In recent simulations another fcc crystal with a substitutional order of the CuAu symmetry was discovered in a narrow window between the CsCl and the tetragonal phases [7].

In addition to the phase transitions found in simulations, a line of continuous phase transitions (λ line) was found in theoretical studies [1,3,8–13], except from the mean-spherical (MSA) and related approximations [1,14,15]. Along the λ line a decay length of a charge-density correlation function, which exhibits exponentially damped oscillations on the length scale $\sim \sigma$, diverges. In some theories the λ line is separated from a first-order transition by a tricritical point (tcp) [8,16–18]. In Ref. [3] this line was just rejected as an unphysical solution. Indeed, a location of the λ line on a phase diagram depends strongly on a regularization of the Coulomb potential inside the hard core [11,19]. This fact may indicate that the λ line is an artifact that results from approximations made in different theories [20,21]. On the other hand, in Ref. [9] it was conjectured that a divergent correlation length is a signature of a crystallization. No quantitative arguments supporting the above conjecture were given, however. Thus, a role of the λ -line in the approximate theories [1,3,8–13] [all of them of a mean-field (MF) type], and its existence in the RPM, remained unclear [1,20].

Renewed interest in the whole phase diagram of the RPM, especially in the λ line and the tcp, is motivated by recent results obtained for the lattice RPM (LRPM), where posi-

tions of ions are restricted to sites of different lattices. On lattices with different symmetries and/or with a lattice constant a corresponding to different values of $\sigma/a \geq 1$, the ions form different periodic patterns at low temperatures T and/or at high densities ρ . Different patterns correspond to different charge-ordered phases. Transitions between the high-temperature, charge-disordered phase and the charge-ordered phases are either continuous or first order, depending on details of a lattice structure [8,12,22–29]. In particular, on a simple cubic (sc) lattice with $\sigma/a=1$, only an order-disorder transition to a phase with two oppositely charged sublattices occurs; this transition is continuous for $T > T_{tc}$, where T_{tc} denotes temperature at the tcp. The phase separation into dilute and dense uniform phases is only metastable [8,10,17,18]. Note that no λ line of continuous transitions is predicted by the MSA for the LRPM [30], in an obvious disagreement with simulations [17,22,27,29] and exact theoretical predictions [30]. The two types of the charge-ordered–charge-disordered transition are shown in Fig. 1. According to recent simulations [4], the transition lines between the liquid and the CsCl crystal are very similar to the thick lines shown in Fig. 1. Note that in contrast to close-packed crystals, the transition density shows significant dependence on temperature.

The above observations raise a question on a relation between the λ line in the continuum space and the charge-ordered–charge-disordered transitions on the lattice. In this work we study effects of fluctuations on the λ line within the field-theoretic description developed in Ref. [8]. On a MF level of this theory the phase diagram for each version of the RPM is the same as on the sc lattice with $\sigma/a=1$ (thin lines in Fig. 1). Namely, only the order-disorder transition that is continuous for $T > T_{tc}$ is present [8,12,25,26]. When fluctuations are included within the field-theoretic approach initiated by Brazovskii [31], in some lattice systems the order-disorder transition becomes fluctuation-induced first order [24–26] (thick lines in Fig. 1). The order of the transition agrees with simulation results for all considered cases [22,27–29]. In Refs. [16,25] arguments were given that in the continuum-space RPM the order-disorder transition becomes fluctuation-induced first order as well.

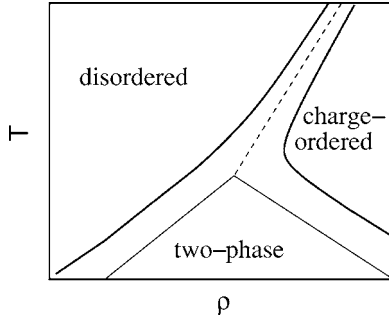


FIG. 1. Schematic representation of the order-disorder transition in the LRPM. Thin dashed- and solid lines represent continuous and first-order transitions respectively that were found on the sc lattice with $\sigma/a=1$ [12,17,22,25,27,29]. The dashed line is a lattice-analog of the λ -line. Thick solid lines represent the first-order transition that occurs for $\sigma/a=\sqrt{2}, 2$ [16,22,25,26,28]. The transition shown by the thin lines can be continuously transformed to the transition shown by the thick lines when additional nearest neighbor repulsion J is present. For small values of J the diagram is shown by the thin lines. When J exceeds a certain value, J_0 , the dashed line splits into two lines that move away when J increases [25,29], and the first-order transition that occurs for large values of J is represented by the thick solid lines. According to simulation results [4], the shape of the liquid-CsCl crystal two-phase region in continuum-space RPM is similar to that shown by the solid lines. Other transitions that occur in some versions of the LRPM and in the continuum space at low- and at high densities are not shown. T and ρ are in arbitrary units.

Except from the order of the considered transition, its location on the phase diagram is of major importance for an identification of the charge-ordered phase. On the MF level of our theory the order-disorder transition occurs at low densities and high temperatures, and the separation into uniform ion-dilute and ion-dense phases is suppressed. Beyond MF, and under the assumption that the order-disorder transition is moved away by fluctuations, the considered field theory [8] predicts that for low densities the phase separation into ion-dilute and ion-dense phases occurs. The associated critical point belongs to the Ising universality class [8,16,32], in agreement with the earlier theoretical arguments by Stell [1,33], and with recent theory [20], experiments [34–36] and simulations [37–42]. It is necessary to verify if the fluctuations may lead to a shift of the phase boundaries of the charge-ordered phase from the phase-space region where the gas-liquid separation takes place, to the phase-space region where the CsCl crystal is stable, to make the field-theoretic arguments in favor of the Ising universality class [8,16,32] complete, and to identify the charge-ordered phase with the CsCl crystal. This is a purpose of our work.

Our work is based on the Brazovskii theory, which turned out to be successful in a description of phase transitions and structure of soft-matter systems [43–45]. Analogous theory for hard crystals has not been developed yet. The important common feature of the soft and ionic crystals is that the periodic ordering is not a result of close packing, but follows directly from interaction potentials, or effective, state-dependent potentials that favor periodic structures for any density. Since the leading physical mechanism that induces

the periodic ordering of soft and ionic crystals is similar, we expect that the Brazovskii approach is an appropriate description of ionic crystallization.

In Sec. II the field-theoretic description of the RPM is described, our approximations are discussed, and notation is fixed. In Sec. III we derive approximate expressions for the grand potential with the fluctuation-contribution included. The following section is devoted to the results obtained for the order-disorder transition. The last section contains a short summary and a discussion.

II. FIELD-THEORETIC DESCRIPTION OF THE RPM

Field theory for the RPM that is considered in this work was derived in Refs. [8,16,26]. In this section we summarize the key steps of the derivation, discuss assumptions and approximations, and fix our notation. We consider local deviations from the uniform number and charge densities, $\eta(\mathbf{x}) = \rho^*(\mathbf{x}) - \rho_0^* = \rho_+^*(\mathbf{x}) + \rho_-^*(\mathbf{x}) - \rho_0^*$ and $\phi(\mathbf{x}) = \rho_+^*(\mathbf{x}) - \rho_-^*(\mathbf{x})$, respectively. $\rho_+^*(\mathbf{x})$ and $\rho_-^*(\mathbf{x})$ correspond to a local number density of cations and anions, respectively, and ρ_0^* is the most probable number density of ions. Asterisks indicate that all densities are dimensionless, and the unit volume is σ^3 , where σ is the core diameter. ϕ is the charge density in e/σ^3 units, e is the charge. We focus on systems that are globally charge neutral,

$$\int_{\mathbf{x}} \phi(\mathbf{x}) = 0, \quad (1)$$

where in this paper we use the notation $\int_{\mathbf{x}} \equiv \int d\mathbf{x}$. Deviations from equilibrium, uniform distributions of ionic species are thermally excited with the probability density [8,16,46]

$$p[\phi, \rho^*] = \Xi^{-1} \exp(-\beta \Omega^{\text{MF}}[\phi, \rho^*]), \quad (2)$$

where Ξ is a normalization constant, and in our theory Ω^{MF} is approximated by [8,16,26]

$$\Omega^{\text{MF}}[\phi, \rho^*] = F_h[\phi, \rho^*] + U[\phi] - \mu \int_{\mathbf{x}} \rho(\mathbf{x}). \quad (3)$$

μ is the chemical potential of the ions, $F_h = \int_{\mathbf{x}} f_h$ is the hard-core reference-system Helmholtz free energy of the mixture in which the core-diameter σ of both components is the same. For the continuum RPM we adopt the Carnahan-Starling (CS) form of f_h in the local-density approximation,

$$\beta f_h(\rho^*, \phi) = \frac{\rho^* + \phi}{2} \ln\left(\frac{\rho^* + \phi}{2}\right) + \frac{\rho^* - \phi}{2} \ln\left(\frac{\rho^* - \phi}{2}\right) - \rho^* + \rho^* \frac{s(4-3s)}{(1-s)^2}, \quad (4)$$

where $\rho^* = \eta + \rho_0^*$, for $\rho^* = \rho_0^*$, the $\Omega^{\text{MF}}[0, \rho^*]$ assumes a minimum, and $s = \pi \rho^* / 6$. Finally, the energy in the RPM is given by

$$\begin{aligned}\beta U[\phi] &= \frac{\beta^*}{2} \int_{\mathbf{x}} \int_{\mathbf{x}'} \theta(|\mathbf{x}' - \mathbf{x}| - 1) \frac{\phi(\mathbf{x}) \phi(\mathbf{x}')}{|\mathbf{x} - \mathbf{x}'|} \\ &= \frac{\beta^*}{2} \int_{\mathbf{k}} \tilde{\phi}(\mathbf{k}) \tilde{V}(k) \tilde{\phi}(-\mathbf{k}),\end{aligned}\quad (5)$$

where $\int_{\mathbf{k}} \equiv \int d\mathbf{k}/(2\pi)^3$. Contributions to the electrostatic energy coming from overlapping cores are not included in (5). We should note that the regularization of the Coulomb potential for $r < \sigma$ is to some extent arbitrary; in particular, in Refs. [11,13,21] different regularizations were chosen. Here and below $x = |\mathbf{x}|$ is measured in σ units. $\beta^* = 1/T^* = \beta e^2/(D\sigma)$ is the inverse temperature in standard reduced units; D is the dielectric constant of the solvent. $\tilde{V}(k) = 4\pi \cos k/k^2$ is the Fourier transform of $V(x) = \theta(x-1)/x$, and k is in σ^{-1} units. From the minimum condition for $\Omega^{\text{MF}}[\phi, \rho^*]$ we obtain the relation between ρ_0^* and the intensive parameters,

$$\beta\mu = \ln \rho_0^* + \frac{s(8 - 9s + 3s^2)}{(1-s)^3}. \quad (6)$$

The fields ϕ and η occur with the probability (2), where the functional $\Omega^{\text{MF}}[\phi, \rho_0^* + \eta]$ consists of a constant term $\Omega^{\text{MF}}[0, \rho_0^*]$ which is irrelevant, and of the term that depends on ϕ and η ,

$$\begin{aligned}\Delta\Omega^{\text{MF}}[\phi, \eta] &= \Omega^{\text{MF}}[\phi, \rho_0^* + \eta] - \Omega^{\text{MF}}[0, \rho_0^*] \\ &= \Omega_2[\phi, \eta] + \Omega_{\text{int}}[\phi, \eta].\end{aligned}\quad (7)$$

The boundary of stability of $\Delta\Omega^{\text{MF}}[\phi, \eta]$ is determined by the Gaussian part,

$$\beta\Omega_2 = \frac{1}{2} \int \frac{d\mathbf{k}}{(2\pi)^3} [\tilde{C}_{\phi\phi}^0(k) \tilde{\phi}(\mathbf{k}) \tilde{\phi}(-\mathbf{k}) + \gamma_{0,2} \tilde{\eta}(\mathbf{k}) \tilde{\eta}(-\mathbf{k})], \quad (8)$$

where

$$\tilde{C}_{\phi\phi}^0(k) = \rho_0^{*-1} + \beta^* \tilde{V}(k), \quad (9)$$

and

$$\gamma_{0,2} = \left. \frac{\partial^2 \beta f_h}{\partial \rho^{*2}} \right|_{\rho^* = \rho_0^*} = \frac{1 + 4s + 4s^2 - 4s^3 + s^4}{(1-s)^4 \rho_0^*}, \quad (10)$$

when the CS reference system is used.

The functional (7) assumes a minimum for the uniform density ρ_0^* and $\phi=0$ as long as its second functional derivative at ρ_0^* and $\phi=0$ is positive definite. The boundary of stability, $\tilde{C}_{\phi\phi}^0(k_b) = 0$, occurs along the line

$$T^* = -\tilde{V}(k_b) \rho_0^* \approx 1.61 \rho_0^*, \quad (11)$$

where $k_b \approx 2.46$ corresponds to the minimum of $\tilde{V}(k)$ [12,16,26]. As the minimum (maximum) of $\Delta\Omega^{\text{MF}}$ corresponds to the maximum (minimum) of the Boltzmann factor (2), $\phi=0$ becomes less probable than $\phi(\mathbf{x}) \propto \cos(\mathbf{r} \cdot \mathbf{k}_b)$ when $T^* < -\tilde{V}(k_b) \rho_0^*$. For temperatures higher than at the line (11) the randomly chosen instantaneous local densities are most

probably uniform. For lower temperatures, however, the randomly chosen instantaneous densities most probably have a form of planar waves with the wave vector \mathbf{k}_b , or of superpositions of such waves. The line (11) separates the regions with and without an instantaneous structure. Hence, for $T^* < -\tilde{V}(k_b) \rho_0^*$ clusters with oppositely charged nearest neighbor are expected to dominate in simulation snapshots.

The last term in Eq. (7) is local, and can be written as

$$\beta\Omega_{\text{int}}[\phi, \eta] = \int_{\mathbf{x}} \beta\omega_{\text{int}}(\phi(\mathbf{x}), \eta(\mathbf{x})), \quad (12)$$

with

$$\beta\omega_{\text{int}}(\phi, \eta) = \sum_{2m+n>2} \frac{\gamma_{2m,n}}{(2m)! n!} \phi^{2m} \eta^n, \quad (13)$$

where $\gamma_{2m,n}$ are appropriate derivatives of βf_h . We consider a truncated form of $\beta\omega_{\text{int}}(\phi, \eta)$, because otherwise analytical results for the fluctuation contribution to the grand potential are not possible. Strictly speaking, the above expansion can be truncated for $\phi \rightarrow 0$ and $\eta \rightarrow 0$. For given values of ϕ and η , in particular for the results of our calculations in the ordered phase, however, the truncated expansion may be oversimplified, especially for small values of ρ_0^* and for large amplitudes of the fields.

In the field theory the grand potential and the charge-density correlation function are given by

$$\Omega = -kT \ln \Xi, \quad (14)$$

and

$$\langle \phi(\mathbf{x}) \phi(\mathbf{x}') \rangle = \Xi^{-1} \int D\eta \int D\phi e^{-\beta\Delta\Omega^{\text{MF}}} \phi(\mathbf{x}) \phi(\mathbf{x}'), \quad (15)$$

respectively, where

$$\Xi = \int D\eta \int D\phi e^{-\beta\Delta\Omega^{\text{MF}}}. \quad (16)$$

In the weighted-field approximation (WF) introduced in Ref. [8], and described in more detail in Refs. [16,26,46], the field $\eta(\mathbf{x})$ is approximated by its most probable form for each given field $\phi(\mathbf{x})$. In other words, for a given field $\phi(\mathbf{x})$, the field $\eta(\mathbf{x})$ is determined by the minimum of $\beta\Delta\Omega^{\text{MF}}[\phi, \eta]$ ($\delta\beta\Delta\Omega^{\text{MF}}[\phi, \eta]/\delta\eta=0$), and can be written in the form

$$\eta_{\text{WF}}[\phi(\mathbf{x})] = \sum_n \frac{a_n}{n!} \phi(\mathbf{x})^{2n}, \quad (17)$$

where the coefficient a_n is given in terms of $\gamma_{2m,j}$ such that $m+j \leq n+1$ [26]. Insertion of $\eta_{\text{WF}}[\phi(\mathbf{x})]$ into Eq. (7) leads to simplified forms of Eqs. (16) and (15),

$$\Xi = \int D\phi e^{-\beta\mathcal{L}_{\text{eff}}(\phi)} \quad (18)$$

and

$$\langle \phi(\mathbf{x}) \phi(\mathbf{x}') \rangle = \Xi^{-1} \int D\phi e^{-\beta \mathcal{H}_{\text{eff}}(\phi)} \phi(\mathbf{x}) \phi(\mathbf{x}'), \quad (19)$$

respectively, where

$$\begin{aligned} \beta \mathcal{H}_{\text{eff}}(\phi) &= \frac{1}{2} \int_{\mathbf{x}} \int_{\mathbf{x}'} \phi(\mathbf{x}) C_{\phi\phi}^0(\mathbf{x} - \mathbf{x}') \phi(\mathbf{x}') \\ &+ \sum_{m=2}^{\infty} \frac{\mathcal{A}_{2m}}{(2m)!} \int_{\mathbf{x}} \phi^{2m}(\mathbf{x}). \end{aligned} \quad (20)$$

The coefficient \mathcal{A}_{2m} is given in terms of $\gamma_{2k,n}$ such that $k+n \leq m$ [26]. For the fluctuation-contribution to the average density we obtain

$$\langle \eta(\mathbf{x}) \rangle = \Xi^{-1} \int D\phi \eta_{\text{WF}}[\phi(\mathbf{x})] e^{-\beta \mathcal{H}_{\text{eff}}(\phi)} = \sum_n \frac{a_n}{n!} \langle \phi(\mathbf{x})^{2n} \rangle. \quad (21)$$

Note that when the expansion in Eq. (20) is truncated at the term $\propto \phi^{2m}$, then in a consistent approximation the expansion in Eq. (21) should be truncated at the term $\propto \langle \phi^{2n} \rangle$ with $n \leq m-1$. Otherwise a_n would contain the coefficients $\gamma_{2k,j}$ that in $\beta \mathcal{H}_{\text{eff}}(\phi)$ are not included.

In this work we shall limit ourselves to the ϕ^6 theory, with \mathcal{H}_{eff} approximated by \mathcal{H}_{WF} of the form

$$\begin{aligned} \beta \mathcal{H}_{\text{WF}}(\phi) &= \frac{1}{2} \int_{\mathbf{x}} \int_{\mathbf{x}'} \phi(\mathbf{x}) C_{\phi\phi}^0(\mathbf{x} - \mathbf{x}') \phi(\mathbf{x}') + \frac{\mathcal{A}_4}{4!} \int_{\mathbf{x}} \phi^4(\mathbf{x}) \\ &+ \frac{\mathcal{A}_6}{6!} \int_{\mathbf{x}} \phi^6(\mathbf{x}). \end{aligned} \quad (22)$$

We should mention that on the sc lattice the above $\mathcal{H}_{\text{WF}}(\phi)$ yields quite good results for the locations of both, the continuous order-disorder transition and the tcp [26]. For the CS reference system the explicit forms of $\mathcal{A}_4, \mathcal{A}_6$ in the WF theory are given in Appendix A. The line of instability of $\mathcal{H}_{\text{WF}}(\phi)$ (λ line) is given in Eq. (11). For stability reasons the expansion in Eq. (20) can be truncated at the term $\sim \phi^{2n_0}$, if the corresponding coupling constant is $\mathcal{A}_{2n_0} > 0$. In the case of the CS reference system we have $\mathcal{A}_4 > 0$ for $\rho_0^* > \rho_{\text{tc}}^* \approx 0.09795$, and $\mathcal{A}_4 < 0$ for $\rho_0^* < \rho_{\text{tc}}^*$. We find $\mathcal{A}_6 > 0$ outside the density interval $\rho_{\text{tc}}^* < \rho_0^* < 0.1541$. Negative coupling constants were also found for the RPM in Ref. [47]. We shall not calculate any quantities for $\rho_{\text{tc}}^* < \rho_0^* < 0.1541$, where the functional (22) is unstable. Near the above range of densities our results are particularly strongly influenced by the lack of the terms $O(\phi^8)$, and are less accurate than elsewhere.

Note that $\tilde{C}_{\phi\phi}^0(k)$ given in Eq. (9) assumes a minimum for $k=k_b > 0$, and can be written in the form

$$\tilde{C}_{\phi\phi}^0(k) = \beta^* [\tau_0 + \Delta \tilde{V}(k)], \quad (23)$$

where

$$\beta^* \tau_0 = \frac{1}{\rho_0^*} + \beta^* \tilde{V}(k_b) \quad (24)$$

and

$$\Delta \tilde{V}(k) = \tilde{V}(k) - \tilde{V}(k_b) \approx_{k \rightarrow k_b} v_2 (k - k_b)^2 + O[(k - k_b)^3]. \quad (25)$$

Near the line of instability of \mathcal{H}_{WF} , we have $\beta^* \tau_0 \rightarrow 0$ [see Eq. (11)]. Because $\tilde{C}_{\phi\phi}^0(k)$ assumes a minimum for $k=k_b$, the fluctuations $\tilde{\phi}(\mathbf{k})$ with $|\mathbf{k}| \approx k_b$ dominate. If the fluctuations with k significantly different from k_b are irrelevant, i.e., for $\tau_0 \ll v_2 k_b^2$ [31], the term $O[(k - k_b)^3]$ in Eq. (25) can be neglected, and

$$\tilde{C}_{\phi\phi}^0(k) \approx \beta^* \tau_0 + \beta^* v_2 (k - k_b)^2. \quad (26)$$

Equations (26) and (22) with $\mathcal{A}_6=0$ are of a similar form as in the Brazovskii theory [31]. In the next section we derive an approximate form for the grand potential in the ϕ^6 theory [Eq. (22) and (26)], by generalizing the Brazovskii approach.

III. CONSTRUCTION OF THE BRAZOVSKII-TYPE APPROXIMATION FOR THE RPM

In the charge-ordered phase characterized by a charge-density profile that is periodic in space, the fluctuating field can be written in the form

$$\phi(\mathbf{x}) = \Phi(\mathbf{x}) + \psi(\mathbf{x}), \quad (27)$$

where

$$\Phi(\mathbf{x}) = \langle \phi(\mathbf{x}) \rangle \quad (28)$$

describes the ordered phase with a particular symmetry. In the ordered phase Eq. (16) can be rewritten in the form

$$\Xi = \exp[-\beta \mathcal{H}_{\text{eff}}(\Phi)] \int D\psi \exp(-\beta \mathcal{H}_{\text{fluc}}[\Phi, \psi]), \quad (29)$$

where

$$\mathcal{H}_{\text{fluc}}[\Phi, \psi] = \mathcal{H}_{\text{eff}}(\Phi + \psi) - \mathcal{H}_{\text{eff}}(\Phi). \quad (30)$$

For the ϕ^6 theory [Eq. (22)] we have

$$\begin{aligned} \beta \mathcal{H}_{\text{fluc}}[\Phi, \psi] &= \frac{1}{2} \int_{\mathbf{x}} \int_{\mathbf{x}'} \psi(\mathbf{x}) C_{\phi\phi}^{\text{fluc}}(\mathbf{x} - \mathbf{x}') \psi(\mathbf{x}') \int_{\mathbf{x}} C_1(\mathbf{x}) \psi(\mathbf{x}) \\ &+ \frac{1}{3!} \int_{\mathbf{x}} C_3(\mathbf{x}) \psi(\mathbf{x})^3 + \frac{1}{4!} \int_{\mathbf{x}} C_4(\mathbf{x}) \psi(\mathbf{x})^4 \\ &+ \frac{1}{5!} \int_{\mathbf{x}} C_5(\mathbf{x}) \psi(\mathbf{x})^5 + \frac{\mathcal{A}_6}{6!} \int_{\mathbf{x}} \psi(\mathbf{x})^6, \end{aligned} \quad (31)$$

where explicit expressions for $C_{\phi\phi}^{\text{fluc}}$ and C_i are given in Appendix B.

By inserting Eq. (29) into Eq. (14) we obtain a functional of the charge-density distribution $\Phi(\mathbf{x})$,

$$-\beta\Omega[\Phi(\mathbf{x})] = -\beta\mathcal{H}_{\text{eff}}[\Phi(\mathbf{x})] + \ln\left(\int D\psi \exp(-\beta\mathcal{H}_{\text{fluc}}[\Phi, \psi])\right). \quad (32)$$

The above equation gives the grand potential in a system with the charge density constrained to have the form $\Phi(\mathbf{x})$. For the theory given by the coarse-grained Hamiltonian (20), or by its truncated version (22), this result is exact. For the charge distribution given by $\Phi(\mathbf{x})$, the first term in Eq. (32) can be directly calculated. In order to obtain an approximation for the fluctuation contribution, we rewrite $\mathcal{H}_{\text{fluc}}[\Phi, \psi]$ in the form

$$\mathcal{H}_{\text{fluc}}[\Phi, \psi] = \mathcal{H}_G[\Phi, \psi] + \Delta\mathcal{H}[\Phi, \psi], \quad (33)$$

where $\mathcal{H}_G[\Phi, \psi]$ is the Gaussian contribution,

$$\mathcal{H}_G[\Phi, \psi] = \frac{1}{2} \int_{\mathbf{x}} \int_{\mathbf{x}'} \psi(\mathbf{x}) C_{\phi\phi}(\mathbf{x} - \mathbf{x}') \psi(\mathbf{x}'). \quad (34)$$

$C_{\phi\phi}(\mathbf{x} - \mathbf{x}')$ is inverse to the exact charge-density correlation function, i.e., in Fourier representation $\tilde{C}_{\phi\phi}(k) = 1/\tilde{G}_{\phi\phi}(k)$, where

$$\tilde{G}_{\phi\phi}(k) = \frac{\delta^2[\beta\Omega(\Phi)]}{\delta\tilde{\Phi}(k)\delta\tilde{\Phi}(-k)}. \quad (35)$$

Next we make an assumption that $\beta\Delta\mathcal{H}[\Phi, \psi]$ can be treated as a small perturbation. When such an assumption is valid, we can write

$$\ln\left(\int D\psi e^{-\beta(\mathcal{H}_G + \Delta\mathcal{H})}\right) \quad (36)$$

$$= \ln\left(\int D\psi e^{-\beta\mathcal{H}_G} \{1 - \beta\Delta\mathcal{H} + O[(\beta\Delta\mathcal{H})^2]\}\right) \\ = \ln \int D\psi e^{-\beta\mathcal{H}_G} + \ln[1 - \langle\beta\Delta\mathcal{H}\rangle_G + O(\langle(\beta\Delta\mathcal{H})^2\rangle_G)], \quad (37)$$

where $\langle\cdots\rangle_G$ denotes averaging with the Boltzmann factor $e^{-\beta\mathcal{H}_G}$. Assuming again that $\langle\beta\Delta\mathcal{H}\rangle_G$ is small, we obtain

$$\beta\Omega(\Phi) = \beta\mathcal{H}_{\text{eff}}(\Phi) - \ln \int D\psi e^{-\beta\mathcal{H}_G} + \langle\beta\Delta\mathcal{H}\rangle_G \\ + O(\langle(\beta\Delta\mathcal{H})^2\rangle_G). \quad (38)$$

In the uniform phase $\beta\Omega$ is given by the same expression, but with $\Phi=0=\beta\mathcal{H}_{\text{eff}}(0)$.

In practice the exact form of $C_{\phi\phi}$ cannot be calculated analytically. In the perturbation theory [48,49] $G_{\phi\phi}$ is given by Feynman diagrams with the $2n$ -point vertices \mathcal{A}_{2n} . The vertices at \mathbf{x} and \mathbf{x}' are connected by lines representing $G_{\phi\phi}^0(\mathbf{x} - \mathbf{x}')$, and all lines are paired. The corresponding expressions are integrated over all vertex points, or in Fourier representation over all $\tilde{G}_{\phi\phi}^0(k)$ line loops. In this work we shall follow the self-consistent, one-loop Hartree

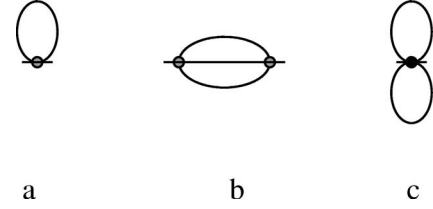


FIG. 2. Feynman diagrams contributing to $C_{\phi\phi}$ in the disordered phase, to two-loop order. Shaded circles and a bullet represent \mathcal{A}_4 and \mathcal{A}_6 , respectively. Lines represent $G_{\phi\phi}^0$. In the self-consistent theory the lines represent $G_{\phi\phi}^H$.

approximation for $\tilde{C}_{\phi\phi}$ [31]. The one-loop contribution to $\tilde{C}_{\phi\phi}$ [Fig. 2(a)] is proportional to $\mathcal{A}_4 \int_{\mathbf{k}} \tilde{G}_{\phi\phi}^0(k)$. In the effectively one-loop ϕ^6 theory (22), another contribution to $\tilde{C}_{\phi\phi}(k)$ is given by a diagram [Fig. 2(c)] that is proportional to $\mathcal{A}_6 [\int_{\mathbf{k}} \tilde{G}_{\phi\phi}^0(\mathbf{k})]^2$ [16,26]. The symmetry factors of the graphs are calculated according to standard rules [48,49]. In the self-consistent, effectively one-loop approximation $\tilde{C}_{\phi\phi}(k)$ assumes the approximate form [16,26,31]

$$\tilde{C}_{\phi\phi}^H(k) = r + \beta^* \Delta \tilde{V}(k), \quad (39)$$

where $r \equiv \tilde{C}_{\phi\phi}^H(k_b)$, and by using (35), (31), and (B1)–(B4) we obtain

$$r = \beta^* \tau_0 + \frac{\mathcal{A}_4 \mathcal{G}(r)}{2} + \frac{\mathcal{A}_6 \mathcal{G}(r)^2}{8} + \frac{1}{2} \left(\mathcal{A}_4 + \frac{\mathcal{A}_6 \mathcal{G}(r)}{2} \right) \int_{\mathbf{x}} \frac{\Phi^2(\mathbf{x})}{V} \\ + \frac{\mathcal{A}_6}{4!} \int_{\mathbf{x}} \frac{\Phi^4(\mathbf{x})}{V}. \quad (40)$$

In the above $V = \int_{\mathbf{x}} 1$ is a volume of the system and

$$\mathcal{G}(r) \equiv \langle \psi(\mathbf{x})^2 \rangle = \int_{\mathbf{k}} \tilde{G}_{\phi\phi}^H(k). \quad (41)$$

The remaining diagrams [including the one shown in Fig. 2(b)] are negligible in the ϕ^4 theory for $\mathcal{A}_4 \sqrt{\beta^*} v_2 k_b \ll r$ [31]. When the above condition is not satisfied, the neglected diagrams, apart from a modification of the form of r , yield additional, k -dependent contribution to $\tilde{C}_{\phi\phi}^H$ in Eq. (39). Inclusion of such contributions goes beyond the scope of this work.

In general, the integral in Eq. (41) cannot be calculated analytically. In fact the integral diverges because of the integrand behavior for $k \rightarrow \infty$. However, the contribution from $k \rightarrow \infty$ is unphysical (overlapping hard cores). When the fluctuations with $k \approx k_b$ dominate ($r \ll \beta^* v_2 k_b^2$), then the main physical contribution to $\mathcal{G}(r)$ comes from $k \approx k_b$. In this case the regularized integral is [31]

$$\mathcal{G}(r) = \int_{\mathbf{k}} \frac{1}{r + \beta^* \Delta \tilde{V}(k)} \simeq_{r \rightarrow 0} \int_{\mathbf{k}} \frac{1}{r + \beta^* v_2 (k - k_b)^2} = \frac{2a\sqrt{T^*}}{\sqrt{r}}, \quad (42)$$

where

$$a = k_b^2 / (4\pi\sqrt{v_2}). \quad (43)$$

Equations (40) and (42) are to be solved self-consistently for the ordered and the disordered phases. In the disordered phase, i.e., for $\Phi=0$, r is denoted by r_0 .

The second term in Eq. (38), with $\tilde{C}_{\phi\phi}(k)$ approximated by $\tilde{C}_{\phi\phi}^H(k)$ [see (39)], is

$$\ln \int D\psi e^{-\beta\mathcal{H}_G} \approx -2a\sqrt{T^*}rV, \quad (44)$$

where the approximation (25) and the same regularization as in the case of Eq. (42) were used. For the last term in Eq. (38) we find [see (33), (31), (39), and (40)]

$$\langle \beta\Delta\mathcal{H} \rangle_G / V = -\frac{\mathcal{G}(r)^2}{8}\mathcal{A}_4 - \frac{\mathcal{G}(r)^3}{24}\mathcal{A}_6 - \frac{\mathcal{G}(r)^2}{16}\mathcal{A}_6 \int_{\mathbf{x}} \frac{\Phi^2(\mathbf{x})}{V}. \quad (45)$$

The above results and Eq. (42) give the explicit form of the grand potential (38),

$$\begin{aligned} \beta\Omega[\rho_0^*, T^*; \Phi; r] / V = & \beta\mathcal{H}_{\text{WF}}[\rho_0^*, T^*; \Phi] / V + 2a\sqrt{rT^*} - \frac{\mathcal{A}_4 a^2 T^*}{2r} \\ & - \frac{\mathcal{A}_6 a^3}{3} \left(\frac{T^*}{r}\right)^{3/2} - \frac{\mathcal{A}_6 a^2 T^*}{4r} \int_{\mathbf{x}} \frac{\Phi^2(\mathbf{x})}{V}, \end{aligned} \quad (46)$$

where $r=r[\rho_0^*, T^*; \Phi]$ is a function of ρ_0^*, T^* and a functional of $\Phi(\mathbf{x})$ that is to be determined from Eqs. (40) and (42). For given values of ρ_0^* and T^* , the value of the (dimensionless) grand potential for a considered phase corresponds to the minimum of $\beta\Omega[\rho_0^*, T^*; \Phi; r]$ with respect to $\Phi(\mathbf{x})$, with ρ_0^* and T^* fixed.

T^* represents temperature, but ρ_0^* differs from the average number density when the fluctuations are included [see (21)]. The lowest-order fluctuation-induced density shift, given by the first term in Eq. (21), yields the leading contribution to the average local density $\rho^*(\mathbf{x})$ of the form

$$\rho_1^*(\mathbf{x}) = \rho_0^* - \frac{\gamma_{2,1}}{2\gamma_{0,2}} [\mathcal{G}(r) + \Phi(\mathbf{x})^2]. \quad (47)$$

The above gives the density shift in the ϕ^4 theory. Higher order terms in Eq. (21) can be included simultaneously with higher-order terms in Eq. (22). In the ϕ^6 theory the next-to-leading order term in Eq. (21) leads to the following approximation for the average density:

$$\rho_2^*(\mathbf{x}) = \rho_1^*(\mathbf{x}) + \frac{a_2}{2} [\Phi(\mathbf{x})^4 + 6\Phi(\mathbf{x})^2\mathcal{G}(r) + 3\mathcal{G}(r)^2], \quad (48)$$

where a_2 is expressed in terms of $\gamma_{2m,n}$ in Appendix A. The thermodynamic density is given by the space-averaged density profile according to

$$\rho^* = \int_{\mathbf{x}} \frac{\rho^*(\mathbf{x})}{V} = \int_{V_u} \frac{\rho^*(\mathbf{x})}{V_u}, \quad (49)$$

where the integration \int_{V_u} is over the unit cell of the ordered structure, and V_u is the unit-cell volume. Explicit expression for the average density in the liquid is given in Appendix A.

In practice a determination of the equilibrium charge-density profile $\Phi(\mathbf{x})$ and the phase transition between the charge-ordered and charge-disordered phases from Eqs. (46), (40), and (42) is difficult. The problem simplifies greatly when a form of $\Phi(\mathbf{x})$ is limited to a particular function that depends on several parameters. In this case the functionals are reduced to functions of several variables, and the problem of obtaining a minimum of $\beta\Omega$ for a given class of functions becomes tractable.

For an ordered phase of a particular symmetry, $\Phi(\mathbf{x})$ can be written as a linear combination of functions $g_i(\mathbf{x})$ forming a corresponding orthonormal basis [44],

$$\Phi(\mathbf{x}) = \sum_i \Phi_i g_i(\mathbf{x}), \quad (50)$$

where Φ_i are the corresponding amplitudes. In Fourier representation the basis functions can be written in the form

$$\tilde{g}_i(\mathbf{k}) = \frac{(2\pi)^d}{\sqrt{2n_i}} \sum_{j=1}^{n_i} [\delta(\mathbf{k} - \mathbf{k}_{ib}^j) + \delta(\mathbf{k} + \mathbf{k}_{ib}^j)], \quad (51)$$

where for the considered symmetry $2n_i$ and \mathbf{k}_{ib}^j are the number of vectors and the j th vector in the i th shell, respectively. In order to specify the structure we need to know the vectors \mathbf{k}_{ib}^j that determine the size of the unit cell of the structure, and the amplitudes Φ_i . We assume that the vectors forming the first shell correspond to the wave vectors of the most probable excitations in the uniform phase. In the theory outlined above such wave vectors are determined by a minimum of $\tilde{C}_{\phi\phi}(k)$, since it yields a maximum of the probability $\propto \exp(-\beta\mathcal{H}_G)$. In the one-loop approximation $\tilde{C}_{\phi\phi}(k)$ assumes a minimum for $|\mathbf{k}|=k_b$, we thus assume $|\mathbf{k}_{ib}^j|=k_b$.

When the form of $\Phi(\mathbf{x})$ is restricted to Eq. (50) and $|\mathbf{k}_{ib}^j|=k_b$, then for given ρ_0^* and T^* , $r=r[\rho_0^*, T^*; \Phi]$ and $\beta\Omega[\rho_0^*, T^*; \Phi; r]$ become functions of the amplitudes Φ_i . Typically, only the first one [31,43] or two shells [44] in Eq. (50) are taken into account in studies of the fluctuation-induced first-order phase transitions [31,43]. Our explicit results are obtained in the one-shell approximation,

$$\Phi(\mathbf{x}) = \Phi_1 g_1(\mathbf{x}). \quad (52)$$

For a few points we also considered the two-shell approximation, but the long formulas will not be given here. In the one-shell approximation we can write

$$\int_{\mathbf{x}} \frac{\Phi(\mathbf{x})^2}{V} = \Phi_1^2, \quad \int_{\mathbf{x}} \frac{\Phi(\mathbf{x})^4}{V} = \Phi_1^4 s_o, \quad \int_{\mathbf{x}} \frac{\Phi(\mathbf{x})^6}{V} = \Phi_1^6 \kappa_o, \quad (53)$$

where

$$s_o = \int_{\mathbf{x}} \frac{g_1(\mathbf{x})^4}{V} = \int_{V_u} \frac{g_1(\mathbf{x})^4}{V_u} \quad (54)$$

and

$$\kappa_o = \int_{\mathbf{x}} \frac{g_1(\mathbf{x})^6}{V} = \int_{V_u} \frac{g_1(\mathbf{x})^6}{V_u}$$

are the geometric factors associated with a particular symmetry of the ordered phase. In the one-shell approximation the above relations should be inserted into Eqs. (40) and (46), and the extremum condition for $\beta\Omega$ can be written in the explicit form

$$r + \left(\mathcal{A}_4 + a\mathcal{A}_6 \sqrt{\frac{T^*}{r}} \right) \left(\frac{s_o}{3!} - \frac{1}{2} \right) \Phi_1^2 + \frac{\mathcal{A}_6}{5!} (\kappa_o - 5s_o) \Phi_1^4 = 0. \quad (55)$$

The resulting set of equations can be solved for each point (ρ_o^*, T^*) with respect to r and Φ_1 . When the results are inserted in Eq. (46), the minimum of the grand potential is obtained for a given pair of s_o and κ_o , i.e., for a chosen structure of the ordered phase. The above method of obtaining the grand potential is equivalent to the method used in Refs. [31,43] and outlined in Appendix D. We verified our calculations by comparing the results obtained by both methods.

IV. TRANSITION BETWEEN THE CHARGE-ORDERED AND CHARGE-DISORDERED PHASES

Let us first focus on the λ line along which the decay length of the charge-density correlation function diverges and the uniform phase becomes unstable. At the boundary of stability of the uniform phase the second functional derivative of the grand-potential functional (38) is $\tilde{C}_{\phi\phi}(k_b)=0$, where k_b is the wave number of the critical charge-density fluctuations. On the MF level, $\tilde{C}_{\phi\phi}(k_b)$ is approximated by $\tilde{C}_{\phi\phi}^0(k_b)$, and the system becomes unstable at the line (11).

In the effectively one-loop self-consistent Hartree approximation $\tilde{C}_{\phi\phi}(k_b)$ is approximated by $\tilde{C}_{\phi\phi}^H(k_b)$. We have found that $\tilde{C}_{\phi\phi}^H(k_b)=r_0$, where r_0 is a self-consistent solution of Eqs. (40) and (41) with $\Phi=0$. For $r_0 \ll 1$ the approximation (42) is valid, and we easily find that $r_0=0$ is a solution of Eqs. (40) and (42) with $\Phi=0$ only for $T^*=0$. Thus, in a presence of fluctuations the λ line of continuous transitions disappears.

For a given thermodynamic state there may exist one or several minima of $\beta\Omega$ [Eq. (46)], associated with a disordered phase and/or ordered phases with different symmetries. The lowest value of the grand potential for given ρ_o^*, T^* corresponds to the stable phase. Other phases are metastable (unstable) if a minimum of the grand potential exists (does not exist). At the phase coexistence two minima of the thermodynamic potential, corresponding to the two coexisting phases, are equal; other minima, if present, are associated with larger values of the grand potential.

When the expansion for $\Phi(\mathbf{x})$ in Eq. (50) is truncated at the first shell, analytical results for the phase coexistence are

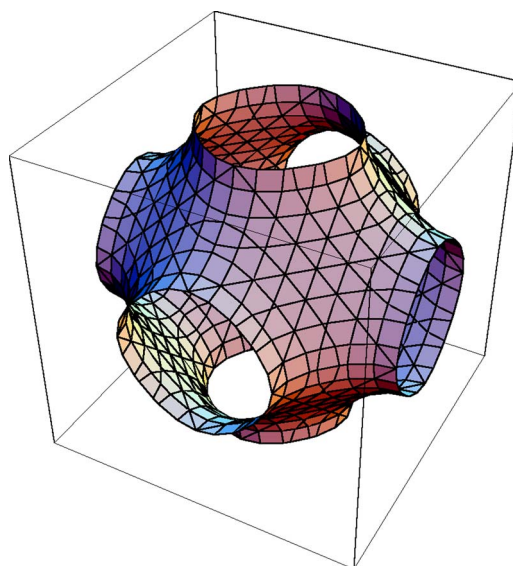


FIG. 3. (Color online) The surface $g_1^P(\mathbf{x})=0$ in the unit cell of the periodic structure P . This surface separates the positively and negatively charged regions. The lattice constant is $2\pi/k_b \approx 2.55$ in ion-diameter units.

possible. However, only a very crude approximation for the ordered structure can be obtained. In this study we shall limit ourselves to analytical calculations in the one-shell approximation. More accurate results for the structure of the ordered phase can be obtained numerically in a future work.

We are interested in a stability of the ionic crystal. In the case of the CsCl symmetry ($Pn3m$), the first shell is formed by the three vectors $\mathbf{k}_b^1/k_b=(1,0,0)$, $\mathbf{k}_b^2/k_b=(0,1,0)$, and $\mathbf{k}_b^3/k_b=(0,0,1)$, i.e., $n_1=3$, and in real space

$$g_1^P(x,y,z) = \frac{2}{\sqrt{6}} [\cos(k_b x) + \cos(k_b y) + \cos(k_b z)]. \quad (56)$$

The above first shell determines the so-called P structure. Unfortunately, topological properties of P differ from that of the CsCl crystal. Namely, the P structure is bicontinuous, i.e., the surface $g_1(\mathbf{x})=0$ separates space into the positively and negatively charged regions, and both regions are continuous, as shown in Fig. 3. In the ionic crystal, however, the positively and negatively charged regions are topologically equivalent to spheres separated by the uncharged solvent of nonvanishing volume. In addition, the nearest neighbor distance in the P structure is $\sqrt{3}\pi/k_b \approx 2.2$. This distance is much larger than in the actual CsCl crystal. The nearest neighbor distance in the ionic crystal is closer to the nearest neighbor distance, $\pi/k_b \approx 1.27$, in the case of the one-dimensional ordering (lamellar phase), where $n_1=1$ and

$$g_1^{\text{lam}}(x) = \sqrt{2} \cos(k_b x). \quad (57)$$

Since the precise structure of the crystalline phase cannot be determined within the one- or two-shell approximation, we consider both phases to find and compare the transition lines between them and the disordered phase. In this way we gain some insight in the approximate location of the actual phase transition.

A. MF approximation

In the MF the fluctuation contribution to $\beta\Omega$ in Eq. (38) is neglected. In the one-shell approximation the grand potential is a function of the amplitude Φ_1 ,

$$\beta\mathcal{H}_{\text{WF}}(\rho_0, T^*, \Phi_1)/V = \frac{1}{2}\beta^* \tau_0 \Phi_1^2 + \frac{\mathcal{A}_4}{4!} s_o \Phi_1^4 + \frac{\mathcal{A}_6}{6!} \kappa_o \Phi_1^6, \quad (58)$$

where the geometric factors s_o and κ_o are found to be

$$s_o = \begin{cases} 3/2, & \text{lamellar structure,} \\ 5/2, & P \text{ structure,} \end{cases} \quad (59)$$

and

$$\kappa_o = \begin{cases} 5/2, & \text{lamellar structure,} \\ 155/18, & P \text{ structure.} \end{cases} \quad (60)$$

For $\rho_0^* > \rho_{\text{tc}}^*$ the order-disorder transition is continuous and coincides with the line of instability (11), whereas for $\rho_0^* < \rho_{\text{tc}}^*$ the order-disorder transition is first order, and occurs when the condition

$$\frac{\partial \beta\mathcal{H}_{\text{WF}}(\rho_0, T^*, \Phi_1)}{\partial \Phi_1} = 0 = \beta\mathcal{H}_{\text{WF}}(\rho_0, T^*, \Phi_1) \quad (61)$$

is satisfied. The expressions for the transition lines T_{lam}^* and T_p^* , and the amplitude Φ_1 are given in Appendix C [Eqs. (C1) and (C2)]. It turns out that the P phase is only metastable. However, the relative difference $(T_{\text{lam}}^* - T_p^*)/T_{\text{lam}}^*$ is very small.

The density in the ordered phase can be obtained from Eq. (47) by neglecting the fluctuation contribution. In the lowest nontrivial order we have

$$\rho^*(\mathbf{x}) = \rho_0^* - \frac{\gamma_{2,1}}{2\gamma_{0,2}} \Phi(\mathbf{x})^2. \quad (62)$$

We verified that Eq. (62) yields $\rho_{\pm}^*(\mathbf{x}) = [\rho^*(\mathbf{x}) \pm \Phi(\mathbf{x})]/2 \geq 0$ for all space positions. The space-averaged density in the ordered phases is given in Eq. (49). The explicit expression for $\Delta\rho^* = \rho^* - \rho_0^*$ is given in Appendix C. The resulting density-temperature phase diagram is shown in Fig. 4.

The diagram shown in Fig. 4 is obtained with the functional $\beta\Delta\Omega^{\text{MF}}[\phi, \eta]$, Eq. (7), approximated by the functional \mathcal{H}_{WF} , Eq. (22). In order to verify the accuracy of the approximation (22), we calculated the functional $\beta\Delta\Omega^{\text{MF}}[\Phi(x), \rho^*(x) - \rho_0^*]$ along the line $T_{\text{lam}}^*(\rho_0^*)$, for the fields $\Phi(x)$ and $\rho^*(x) - \rho_0^*$ that yield $\mathcal{H}_{\text{WF}} = 0$. The result shown in Fig. 5 indicates that our approximate functional (22) yields the poorest accuracy in this part of the phase diagram where \mathcal{A}_6 is very small [see the discussion below Eqs. (13) and (22)], and the term $\propto \phi^8$ should be included. We also considered the two-shell approximation for $\Phi(\mathbf{x})$. We found very similar results, with somewhat lower transition temperatures, and with a smaller difference between them. We conclude that the transition temperature obtained in the approximate theory [Eq. (22)] is overestimated.

Our main concern in this work is to determine the fluctuation contribution to the grand potential in Eq. (38). We

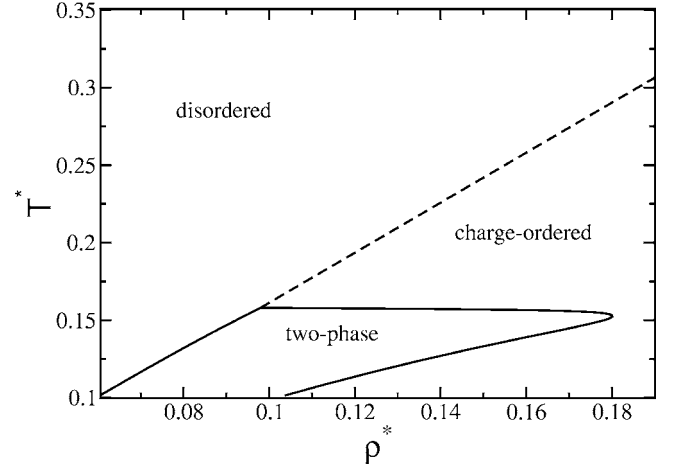


FIG. 4. Density-temperature MF phase diagram obtained from the approximate functional (58). Temperature T^* and density ρ^* are in standard reduced units defined in Sec. II.

shall not attempt to find better MF results by numerical minimization of the functional (7).

B. Effects of fluctuations on phase transitions

In this section we include the fluctuation contribution to Ω in Eq. (38). We consider two cases, the ϕ^4 theory ($\mathcal{A}_6 \equiv 0$ in the above equations), as in the Brazovskii work [31], and the ϕ^6 theory.

1. Results of the ϕ^4 theory

The ϕ^4 theory is stable for $\rho_0^* > \rho_{\text{tc}}^*$, and for such densities the term $O(\phi^6)$ can be neglected. In this case analytical solutions for r_0 and r of Eqs. (40) and (55) can be obtained. Physical solution for r corresponds to the lowest value of Φ_1 . The transition lines between the uniform and the two ordered phases are shown in Fig. 6. In the one-shell approximation

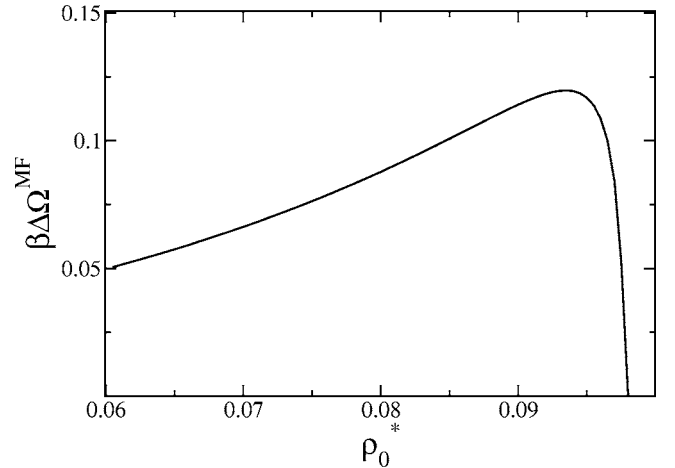


FIG. 5. The MF grand potential $\beta\Delta\Omega^{\text{MF}}[\Phi(\mathbf{x}), \rho^*(\mathbf{x}) - \rho_0^*]$ [see Eq. (7)] along the approximate transition line (C1), where $\mathcal{H}_{\text{WF}} = 0$. $\Phi(\mathbf{x})$ and $\rho^*(\mathbf{x})$ are given in Eq. (52) with (C2), and in Eq. (62), respectively.

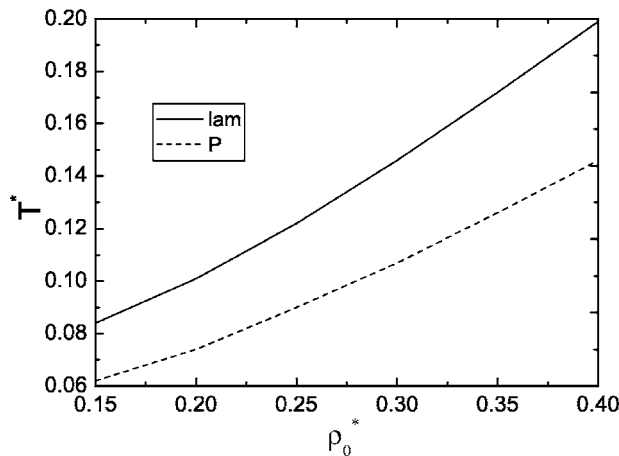


FIG. 6. The fluctuation-induced first-order transition lines between the disordered and the ordered phases in the ϕ^4 theory in the (ρ_0^*, T^*) phase diagram. The transition to the P phase is metastable.

the lamellar order turns out to be more stable than the P phase. We also considered the much more tedious two-shell approximation for a few points. We found Φ_2 significantly smaller than Φ_1 , and the phase-transition lines shifted to somewhat lower temperatures compared to the one-shell approximation. The rest of our results is obtained in the much simpler one-shell approximation.

Recall that our results rely on the approximate Eq. (42), which is valid provided that the condition $r \ll v_2 k_b^2 / T^*(\rho_0^*)$ is satisfied. We verified that along the coexistence lines $T^*(\rho_0^*)$ (Fig. 6), the r and r_0 are one and two orders of magnitude smaller than $v_2 k_b^2 / T^*(\rho_0^*) \approx 6 / T^*(\rho_0^*)$, respectively. Thus, close to the phase coexistence the approximation (42) used in our calculations is valid. However, the condition $\mathcal{A}_4 \sqrt{\beta^*} v_2 k_b \ll r$, under which the disregarded diagrams [including Fig. 2(b)] can be neglected [31], is not satisfied for low densities. Since \mathcal{A}_4 decreases with increasing density, for higher densities the accuracy of our results improves.

In Fig. 7 the temperature at the transition to the lamellar phase is shown as a function of the most probable density (MF result) and as a function of the average density, given by the approximate expressions (47) and (A7). The average density is a nonmonotonic function of T^* along the phase coexistence (Fig. 7) for $T^* < 0.15$. As already discussed in Sec. III, for the corresponding range of ρ_0^* the approximate functional (22) is oversimplified. Moreover, the neglected diagrams [Fig. 2(b)] may yield a relevant contribution to the grand potential for low densities.

Let us compare the temperatures at the continuous transition in MF and at the first-order transition in our theory (Figs. 4 and 7). In particular, for $\rho^* = 0.8$ we find $T^* \approx 1.29$ and $T^* \approx 0.43$ in the first and in the second case, respectively. For $T^* \approx 0.43$, on the other hand, we find in MF the transition density $\rho_0^* \approx 0.28$, a much lower value than in our theory. As we see, in this approximation the fluctuation-induced shift of the liquid-phase boundary is substantial. However, for $\rho^* = 0.8$ the temperature at the transition between liquid and the CsCl crystal obtained in simulations [4] is $T^* \approx 0.1$. Before we identify the charge-ordered phase, we need to find out how the transition temperature and density change when

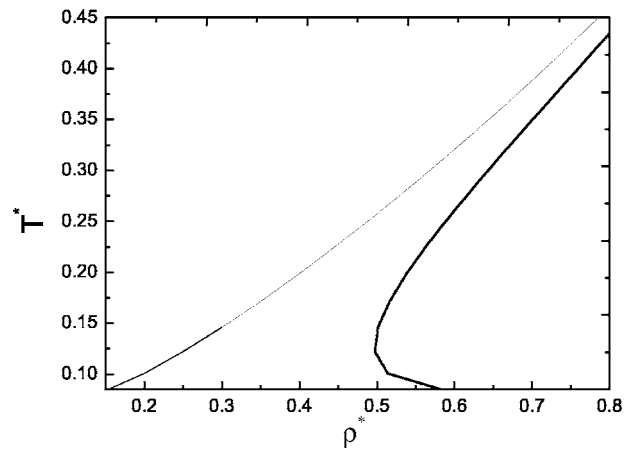


FIG. 7. Temperature at the liquid-lamellar phase transition in the ϕ^4 theory as a function of the average density in the liquid phase at different levels of approximation in Eq. (21). Thin solid line corresponds to the zeroth-order term in Eq. (21), i.e., ρ^* is approximated by ρ_0^* . Thick solid line is obtained by including the leading-order contribution to the fluctuation-induced density shift, i.e., ρ^* is approximated by ρ_1^* [Eq. (47)]. Explicit expression for the average density in the liquid is given in Eq. (A7).

better approximations for \mathcal{H}_{WF} , for the function $\Phi(\mathbf{x})$ and for the average density are made within our theory. In the next section we study the role of the ϕ^6 term in Eq. (22).

2. Results of the ϕ^6 theory

In this section we determine the effect of the ϕ^6 term on the phase behavior. Analytical solutions for the phase transitions can be obtained by using the original Brazovskii method [31,43], if in equations determining the phase transition the terms of the highest order in Φ_1 are neglected. This is justified when $\Phi_1 \ll 1$. In Appendix D we explain the key steps of the calculations. The full equations in the ϕ^6 theory can only be solved numerically. Results for the transition lines between the uniform and the two ordered phases are shown in Fig. 8, where analytical results of the approximate theory and numerical results of the full ϕ^6 theory are shown as lines and as symbols, respectively. The liquid-phase boundary, $T^*(\rho_0^*)$, is shown in Fig. 9 as a function of the average density at different levels of approximation in Eq. (21). The thick solid line is obtained from Eq. (21) with the two leading-order terms included, i.e., in an approximation consistent with Eq. (22). We verified that Eq. (42) used in our calculations is also valid in the ϕ^6 theory.

By comparing Figs. 6 and 8 we see that in the ϕ^6 theory both transition lines are significantly shifted to lower temperatures compared to the ϕ^4 theory. Figure 9 shows that in the consistent approximation for the average density, higher density at the phase coexistence is obtained. The results of the ϕ^6 theory are thus closer to the simulation results for the liquid-CsCl transition, but the transition temperatures are still too high. For example, for $\rho^* = 0.8$ we have $T^* \approx 0.43$ and $T^* \approx 0.28$ in the ϕ^4 and in the ϕ^6 theory, respectively, whereas for the liquid-CsCl transition $T^* \approx 0.1$ for the same density [4]. Note that the MF results (see the discussion at the end of Sec. IV A) suggest that the truncated functional

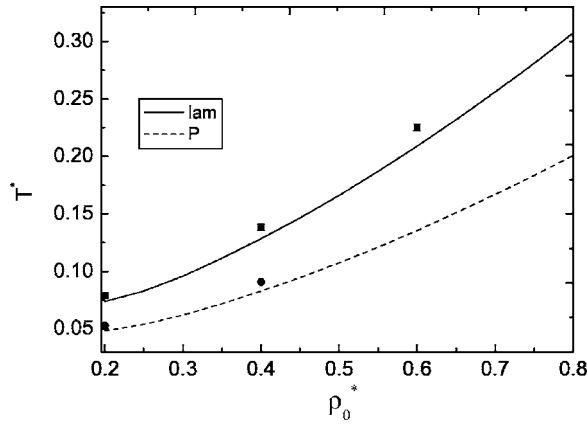


FIG. 8. The fluctuation-induced first-order transition lines between the liquid and the ordered phases in the ϕ^6 theory in the (ρ_0^*, T^*) phase diagram. Lines are the analytical solutions of the approximate equations (Appendix D) and symbols are the numerical solutions of the full equations described in the text. The transition to the P phase is metastable.

(22) leads to overestimated transition temperatures compared to the original functional (7). We can expect that by addition of the term $\sim \phi^8$ in Eq. (22) and the third-order term in Eq. (21), lower temperatures and higher densities at the transition should be obtained. Better forms of the charge-density profile $\Phi(\mathbf{x})$ should lead to lower transition temperatures as well, as indicated by the (partial) results that we obtained in the two-shell approximation. Thus, systematic improvement of the approximations that we make in explicit calculations, should lead to systematically decreasing transition temperature and increasing density, and our results should systematically approach the simulation results for the liquid–ionic-crystal transition [4].

For the two quite different charge-ordered phases the transitions to the disordered phase are not far from each other

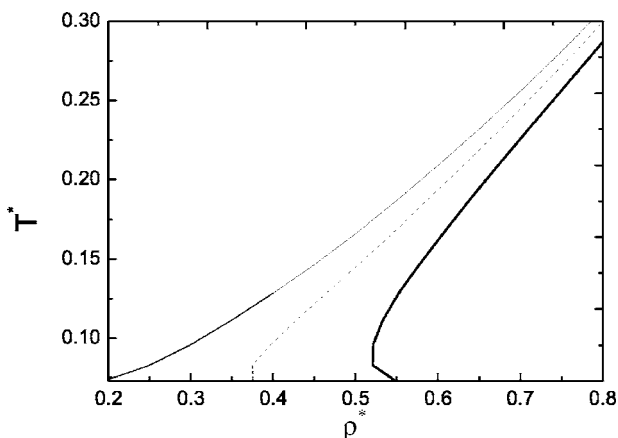


FIG. 9. Temperature at the first-order phase transition between liquid and the charge-ordered phase in the ϕ^6 theory, as a function of the average density (21) at different levels of approximation. Thin solid line corresponds to ρ^* approximated by the MF result, ρ_0^* . Along the dashed line ρ^* is given by the space-averaged leading-order fluctuation contribution to the average density ρ_1^* [Eq. (47)]. Thick solid line corresponds to ρ_2^* [Eq. (48)], where the next-to-leading ordered term in (21) is taken into account.

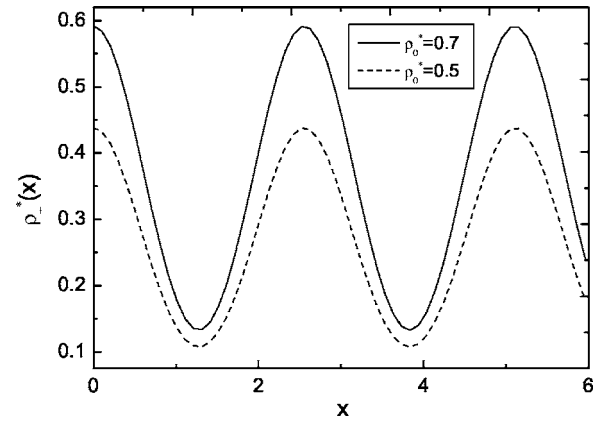


FIG. 10. The density profiles of cations, $\rho_+^*(x)$, in the charge-ordered phase at the coexistence with the liquid phase for two different densities in the ϕ^6 theory. Dashed line corresponds to $\rho_0^*=0.5$ ($\rho^* \approx 0.6$) and the solid line corresponds to $\rho_0^*=0.7$ ($\rho^* \approx 0.75$). x is in σ units and ρ_+^* is dimensionless.

(Fig. 8). It is thus plausible that the transitions to the other ordered structures, including the stable one, are located in the same part of the phase diagram.

Let us focus on the density difference between the coexisting phases. In the high-temperature part of the phase coexistence the density difference $\Delta\rho^*$ between the coexisting phases is rather small (see Ref. [4] and Fig. 1). By using Eqs. (49) and (48) we find a vanishingly small density difference between the coexisting liquid and lamellar phases. This result probably follows from the poor, one-shell ansatz for the charge-density profile. The density profile of cations, $\rho_+^*(x) = [\rho_2^*(x) + \Phi(x)]/2$, where $\rho_2^*(x)$ is given in Eq. (48), is shown in Fig. 10 for two densities at the coexistence with the liquid phase. Beyond the effective one-loop approximation we expect some dependence of the unit cell of the crystal on density, but its determination requires further studies. The shape of the density profile in the charge-ordered phase resembles an average density profile in a crystal (but only in one direction). Of course in the one-shell approximation the crystalline structure cannot be reproduced accurately. Our results for the liquid phase are more accurate, because they do not depend on the form of $\Phi(\mathbf{x})$, which is the weakest point of our explicit results.

V. SUMMARY

In this work we considered the fluctuation contribution to the grand-thermodynamic potential in Eq. (32) within the field-theoretic description of the RPM. Our main purpose was a determination of an order, location and nature of the transition between the charge-disordered and charge-ordered phases. We obtained an approximate expression [Eqs. (46), (40), and (42)] for the grand-potential functional of the charge-density profile $\Phi(\mathbf{x})$ in the ordered phase. Our approximation is based on the self-consistent, effective one-loop Hartree approximation, applied to the ϕ^6 theory that was derived for the RPM in Ref. [26].

We found that in the continuum-space RPM the λ line of continuous transitions disappears when the charge-density

fluctuations are included. Instead, a first-order transition to a charge-ordered phase appears. The range of temperatures and densities at the first-order transition to the charge-ordered phase is similar to the range of temperatures and densities at the liquid–ionic-crystal transition found in simulations [4]. In the charge-ordered phase the average charge-density exhibits oscillations with a period $\sim 2.5\sigma$ (beyond the one-loop approximation the period may be slightly different), and with an amplitude ~ 0.5 . Thus, our results strongly indicate that the fluctuation-induced first-order order-disorder transition should be identified with ionic crystallization. We can conclude that the λ line found in different theories of the MF type is in fact a MF indication of ionic crystallization. We should note, however that the line (11) plays a role of a structural line. At the low-temperature side of this line instantaneous density profiles of a form of charge-density waves with a period $\sim 2.5\sigma$ dominate. In real space charge-ordered clusters are formed, and individual ions are rare in typical microscopic states (simulation snapshots). The structure of typical microscopic states changes continuously when the high temperature side of the line (11) is approached, and random distribution of charges begin to dominate at the high T^* side of the line (11). The densities of ions averaged over all microscopic states are uniform on both sides of the structural line (11) when fluctuations are included.

The explicit results for the first-order phase transition were obtained analytically within the simplest, one-shell approximation for $\Phi(\mathbf{x})$ [see (52)], for two ordered structures: one-dimensional, lamellar phase, and three-dimensional, P phase shown in Fig. 3. We do not expect that the structure of the charge-ordered phase can be correctly reproduced on this simple level of approximation. Our approximate result for the crystalline structure is only a very crude approximation. The transition lines for the two different structures, however, are located close to each other on the (ρ^*, T^*) phase diagram. It is thus very plausible that the transition line to the stable phase should be located near the two transition lines, and conclusions concerning the approximate location of the order-disorder transition are justified.

In the effectively one-loop approximation we find the same lattice constant of the CsCl crystal, $2\pi/k_b$, for a range of densities. Beyond the one-loop approximation we expect a weak dependence of the lattice constant on density. This result and Fig. 10 suggest that the number of defects (vacancies) in the crystal coexisting with the liquid (fused salt) increases with decreasing T^* . The crystal melts either when at relatively low T^* many defects are present (low ρ^*), or when there are only few defects (high ρ^*), but T^* is high.

Our results show a reasonable agreement with simulations even for the very crude approximation for $\Phi(\mathbf{x})$, and we verified that by addition of further terms to Eqs. (22), (47), and (52) a better agreement should be obtained. The accuracy of the results can be significantly improved within the approach developed in this work by choosing a better ansatz for the form of $\Phi(\mathbf{x})$. Note that the fluctuation contribution to $\beta\Omega$ depends only on global characteristics of $\Phi(\mathbf{x})$, i.e., on integrals of $\Phi(\mathbf{x})^{2n}$, where $n \leq 3$ in the case of the ϕ^6 theory. Only the MF contribution depends on adetailed shape of $\Phi(\mathbf{x})$ through the term $\int_{\mathbf{x}} \int_{\mathbf{x}'} \Phi(\mathbf{x}) C_{\phi\phi}^0(\mathbf{x}-\mathbf{x}') \Phi(\mathbf{x}')$

$= \int_{\mathbf{k}} \tilde{\Phi}(\mathbf{k}) \tilde{C}_{\phi\phi}^0(\mathbf{k}) \tilde{\Phi}(\mathbf{k}')$. Numerical determination of the structure of the charge-ordered phase is thus possible within our approach, but it goes beyond the scope of the present work. We conclude that the field-theoretic approach developed in this work is suitable for a description of ionic crystallization on a semiquantitative level.

ACKNOWLEDGMENTS

This work was supported by the KBN through a research project 1 P02B 033 26.

APPENDIX A: COEFFICIENTS \mathcal{A}_4 , \mathcal{A}_6 , AND a_2 IN THE WF APPROXIMATION

The coupling constants in the WF approximation are given in terms of the coefficients $\gamma_{2m,n}$ [26],

$$\mathcal{A}_4 = \gamma_{4,0} - 3 \frac{(-\gamma_{2,1})^2}{\gamma_{0,2}}, \quad (\text{A1})$$

$$\begin{aligned} \mathcal{A}_6 = & \gamma_{6,0} - 15 \frac{(-\gamma_{2,1})(-\gamma_{4,1})}{\gamma_{0,2}} - 15 \frac{(-\gamma_{2,1})^3(-\gamma_{0,3})}{\gamma_{0,2}^3} \\ & - 45 \frac{(-\gamma_{2,2})(-\gamma_{2,1})^2}{\gamma_{0,2}^2}, \end{aligned} \quad (\text{A2})$$

and in the CS approximation they assume the explicit forms

$$\mathcal{A}_4 = - \frac{1 - 20s + 10s^2 - 4s^3 + s^4}{\rho_0^{*3}(1 + 4s + 4s^2 - 4s^3 + s^4)} \quad (\text{A3})$$

and

$$\mathcal{A}_6 = \frac{3W(s)}{\rho_0^{*5}(1 + 4s + 4s^2 - 4s^3 + s^4)^5}, \quad (\text{A4})$$

where

$$\begin{aligned} W(s) = & 3 - 84s + 360s^2 + 2644s^3 + 1701s^4 - 8736s^5 \\ & + 11\,240s^6 - 8304s^7 + 3861s^8 - 1164s^9 + 240s^{10} \\ & - 36s^{11} + 3s^{12}. \end{aligned}$$

The coefficient a_2 in Eqs. (21) and (48) is

$$\frac{a_2}{2} = - \frac{\Gamma_{4,1}^0}{4! \gamma_{0,2}}, \quad (\text{A5})$$

where

$$\Gamma_{4,1}^0 = \gamma_{4,1} - \frac{6(-\gamma_{2,2})(-\gamma_{2,1})}{\gamma_{0,2}} - \frac{3(-\gamma_{3,0})(-\gamma_{2,1})^2}{\gamma_{0,2}^2}. \quad (\text{A6})$$

In the liquid phase the explicit form of the average density (47) is

$$\rho_1^* = \rho_0^* + \frac{a(1-s)^4}{\rho_0^*(1 + 4s + 4s^2 - 4s^3 + s^4)} \sqrt{\frac{T^*}{r_0}}, \quad (\text{A7})$$

where Eq. (42), Eq. (40) with $\Phi=0$, and the CS reference system have been used. The explicit form of ρ_2^* can be

obtained in the same way with the help of Eqs. (A5) and (A6).

APPENDIX B: EXPLICIT FORMS OF THE FUNCTIONS $C_{\phi\phi}^{\text{fluc}}$ AND C_i IN THE FUNCTIONAL (31)

$$C_{\phi\phi}^{\text{fluc}}(\mathbf{x} - \mathbf{x}') = C_{\phi\phi}^0(\mathbf{x} - \mathbf{x}') + \left(\frac{\mathcal{A}_4}{2!} \Phi^2(\mathbf{x}) + \frac{\mathcal{A}_6}{4!} \Phi^4(\mathbf{x}) \right) \times \delta(\mathbf{x} - \mathbf{x}'), \quad (\text{B1})$$

$$C_1(\mathbf{x}) = \int_{\mathbf{y}} \Phi(\mathbf{y}) C_{\phi\phi}^0(\mathbf{y} - \mathbf{x}) + \frac{\mathcal{A}_4}{3!} \Phi^3(\mathbf{x}) + \frac{\mathcal{A}_6}{5!} \Phi^5(\mathbf{x}), \quad (\text{B2})$$

$$C_3(\mathbf{x}) = \mathcal{A}_4 \Phi(\mathbf{x}) + \frac{\mathcal{A}_6}{6} \Phi(\mathbf{x})^3, \quad (\text{B3})$$

$$C_4(\mathbf{x}) = \mathcal{A}_4 + \frac{\mathcal{A}_6}{2} \Phi(\mathbf{x})^2, \quad (\text{B4})$$

and

$$C_5(\mathbf{x}) = \Phi(\mathbf{x}). \quad (\text{B5})$$

APPENDIX C: EXPLICIT EXPRESSIONS FOR THE PHASE TRANSITIONS IN THE MF APPROXIMATION

The line of the first-order transition and the amplitude of the charge-density wave are given by

$$T^* = \frac{8\mathcal{A}_6\kappa_o \tilde{V}(k_b) \rho_0^*}{5(\mathcal{A}_4 s_o)^2 \rho_0^* - 8\mathcal{A}_6\kappa_o} \quad (\text{C1})$$

and

$$\Phi_1^2 = -\frac{\mathcal{A}_4 s_o}{\mathcal{A}_6 \kappa_o}, \quad (\text{C2})$$

respectively. The space-averaged density shift has the form

$$\Delta\rho^* = \frac{15\gamma_{2,1}\mathcal{A}_4 s_o^{\text{lam}}}{2\gamma_{0,2}\mathcal{A}_6 \kappa_o^{\text{lam}}}. \quad (\text{C3})$$

APPENDIX D: EXPLICIT EXPRESSION FOR THE GRAND-POTENTIAL DIFFERENCE

After a substitution of Eqs. (27) and (28) into Eq. (22), the Brazovskii's equation of state [22],

$$h = \frac{\delta\Omega}{\delta\tilde{\Phi}(\mathbf{k}_b)},$$

can be written as

$$h = \left(\tilde{C}_{\phi\phi}^0(\mathbf{k}_b) + \frac{\mathcal{A}_4\mathcal{G}}{2} + \frac{\mathcal{A}_6\mathcal{G}^2}{8} \right) \tilde{\Phi}(-\mathbf{k}_b) + \left(\frac{\mathcal{A}_4}{3!} + \frac{\mathcal{A}_6}{12}\mathcal{G} \right) \int_{\mathbf{k}'} \int_{\mathbf{k}''} \int_{\mathbf{k}'''} \delta(\mathbf{k}_b + \mathbf{k}' + \mathbf{k}'' + \mathbf{k}''') \times \tilde{\Phi}(\mathbf{k}') \tilde{\Phi}(\mathbf{k}'') \tilde{\Phi}(\mathbf{k}''') + \frac{\mathcal{A}_6}{5!} \int_{\mathbf{k}'} \int_{\mathbf{k}''} \int_{\mathbf{k}'''} \int_{\mathbf{k}''''} \int_{\mathbf{k}'''''} \delta(\mathbf{k}_b + \mathbf{k}' + \mathbf{k}'' + \mathbf{k}''' + \mathbf{k}'''' + \mathbf{k}''''') \prod_i \tilde{\Phi}(\mathbf{k}^i), \quad (\text{D1})$$

where $\tilde{C}_{\phi\phi}^0(\mathbf{k})$ and \mathcal{G} are given in Eqs. (26) and (43), respectively. For $\tilde{C}_{\phi\phi}(k)$ [see Eq. (27)] we obtain Eq. (39) with (40).

For $|\Phi| \ll 1$ we truncate the expansions in Φ in Eqs. (D1) and (40) at the $O(\Phi^3)$ and $O(\Phi^2)$ terms, respectively. As a result, the correlation function is given in Eq. (40) with the term $O(\Phi^4)$ neglected. The truncated Eq. (D1), and Eq. (40) give for h the result

$$h = r\tilde{\Phi}(-\mathbf{k}_b) + \left(\mathcal{A}_4 + \frac{\mathcal{A}_6\mathcal{G}}{2} \right) \int_{\mathbf{k}_1} \int_{\mathbf{k}_2} \tilde{\Phi}(\mathbf{k}_1) \tilde{\Phi}(\mathbf{k}_2) \times \left(\frac{1}{3!} \tilde{\Phi}(\mathbf{k}_b - \mathbf{k}_1 - \mathbf{k}_2) - \frac{1}{2} \tilde{\Phi}(\mathbf{k}_b) \right). \quad (\text{D2})$$

In the one-shell approximation the explicit form of the equilibrium condition $h=0$ is

$$r + \left(\mathcal{A}_4 + \frac{\mathcal{A}_6\alpha}{\sqrt{r}} \right) b_n \Phi_1^2 = 0, \quad (\text{D3})$$

where $\alpha = a\sqrt{T^*}$, with a given in Eq. (43), and

$$b_n = \frac{\sqrt{2n_1}}{3!} \int_{\mathbf{k}_1} \int_{\mathbf{k}_2} \tilde{g}_1(\mathbf{k}_1) \tilde{g}_1(\mathbf{k}_2) \tilde{g}_1(\mathbf{k}_b - \mathbf{k}_1 - \mathbf{k}_2) - \frac{1}{2}. \quad (\text{D4})$$

For both the lamellar and P structures $b_n = -1/(4n_1)$.

The difference between the thermodynamic potential in the ordered and the disordered phases can be obtained in the same way as in Ref. [43], and we find

$$\Delta\Omega = \frac{\mathcal{A}_4 b_n}{4} \Phi_1^4 + \Omega_r, \quad (\text{D5})$$

where

$$\Omega_r = \int_0^{\Phi_1} d\varphi \varphi \left(r + \frac{\mathcal{A}_6 b_n \alpha}{\sqrt{r}} \varphi^2 \right), \quad (\text{D6})$$

$$\varphi^2 = \frac{2r^{3/2} - 2\sqrt{r}\beta^* \tau_0 - \mathcal{A}_4 \alpha}{\mathcal{P}} - \frac{\alpha}{\sqrt{r}}, \quad (\text{D7})$$

and

$$\varphi d\varphi = \left(\frac{\sqrt{r}}{\mathcal{P}} + \frac{\alpha}{2r^{3/2}} + \frac{\mathcal{A}_6\alpha\varphi^2}{2r\mathcal{P}} \right) dr, \quad \mathcal{P} = \mathcal{A}_4\sqrt{r} + \mathcal{A}_6\alpha. \quad (\text{D8})$$

After inserting (D7) and (D8) into (D6) we obtain an integral which can be calculated analytically (with the

help of Mathematica). In order to obtain r and Φ_1 at the coexistence, we solve Eq. (40) supplemented with the condition (D3). As a result, we arrive at the explicit expressions for $\Delta\Omega$ and r , which were used in a determination of the phase diagram shown in Fig. 9, but are too cumbersome to be presented here.

-
- [1] G. Stell, *J. Stat. Phys.* **78**, 197 (1995).
 [2] M. E. Fisher, *J. Stat. Phys.* **75**, 1 (1994).
 [3] F. H. Stillinger, J. G. Kirkwood, and P. J. Wojtowicz, *J. Chem. Phys.* **32**, 1837 (1960).
 [4] C. Vega, J. L. F. Abascal, C. McBride, and F. Bresme, *J. Chem. Phys.* **119**, 964 (2003).
 [5] B. Smit, K. Esselink, and D. Frenkel, *Mol. Phys.* **87**, 159 (1996).
 [6] F. Bresme, C. Vega, and J. L. F. Abascal, *Phys. Rev. Lett.* **85**, 3217 (2000).
 [7] A. P. Hynninen, M. E. Leunissen, A. van Blaaderen, and M. Dijkstra, *Phys. Rev. Lett.* **96**, 018303 (2006).
 [8] A. Ciach and G. Stell, *J. Mol. Liq.* **87**, 253 (2000).
 [9] C. Outhwaite, in *Statistical Mechanics. A Specialist Periodic Report*, edited by K. Singer (The Chemical Society, London, 1975), Vol. 2, p. 188.
 [10] G. Stell, in *New Approaches to Problems in Liquid-State Theory*, edited by C. Caccamo, J.-P. Hansen, and G. Stell (Kluwer Academic, Dordrecht, 1999).
 [11] O. Patsahan and I. Mryglod, *Condens. Matter Phys.* **7**, 755 (2004).
 [12] A. Ciach and G. Stell, *J. Chem. Phys.* **114**, 3617 (2001).
 [13] O. Patsahan, *Condens. Matter Phys.* **7**, 35 (2004).
 [14] R. L. de Carvalho and R. Evans, *J. Phys.: Condens. Matter* **7**, 575 (1995).
 [15] R. L. de Carvalho and R. Evans, *Mol. Phys.* **83**, 619 (1994).
 [16] A. Ciach and G. Stell, *Int. J. Mod. Phys. B* **21**, 3309 (2005).
 [17] R. Dickman and G. Stell, in *Simulation and Theory of Electrostatic Interactions in Solution*, edited by L. Pratt and G. Hummer, AIP Conf. Proc. 492 (American Institute of Physics, Melville, NY, 1999).
 [18] V. Kobelev, A. B. Kolomeisky, and M. Fisher, *J. Chem. Phys.* **117**, 8897 (2002).
 [19] A. Ciach, W. T. Gózdź, and R. Evans, *J. Chem. Phys.* **118**, 3702 (2003).
 [20] O. Patsahan and I. Mryglod, *J. Phys.: Condens. Matter* **16**, L235 (2004).
 [21] J. M. Caillol, *J. Stat. Phys.* **115**, 1461 (2004).
 [22] A. Z. Panagiotopoulos and S. K. Kumar, *Phys. Rev. Lett.* **83**, 2981 (1999).
 [23] A. Ciach and G. Stell, *J. Chem. Phys.* **114**, 382 (2001).
 [24] A. Ciach and G. Stell, *Phys. Rev. Lett.* **91**, 060601 (2003).
 [25] A. Ciach and G. Stell, *Phys. Rev. E* **70**, 016114 (2004).
 [26] A. Ciach, *Phys. Rev. E* **70**, 046103 (2004).
 [27] A. Diehl and A. Z. Panagiotopoulos, *J. Chem. Phys.* **118**, 4993 (2003).
 [28] A. Diehl and A. Z. Panagiotopoulos, *J. Chem. Phys.* (to be published).
 [29] A. Diehl and A. Z. Panagiotopoulos, *Phys. Rev. E* **71**, 046118 (2005).
 [30] J. Hoye and G. Stell, *J. Stat. Phys.* **89**, 177 (1997).
 [31] S. A. Brazovskii, *Sov. Phys. JETP* **41**, 8 (1975).
 [32] A. Ciach, e-print cond-mat/0601052.
 [33] G. Stell, *Phys. Rev. A* **45**, 7628 (1992).
 [34] W. Schröer, M. Wagner, and O. Stanga (unpublished).
 [35] M. Kleemeier, S. Wiegand, W. Schröer, and H. Weingärtner, *J. Chem. Phys.* **110**, 3085 (1999).
 [36] S. Wiegand *et al.*, *J. Chem. Phys.* **109**, 9038 (1998).
 [37] Y. C. Kim, M. E. Fisher, and E. Luijten, *Phys. Rev. Lett.* **91**, 065701 (2003).
 [38] G. Orkoulas and A. Z. Panagiotopoulos, *J. Chem. Phys.* **110**, 1581 (1999).
 [39] Q. Yan and J. J. de Pablo, *J. Chem. Phys.* **111**, 9509 (1999).
 [40] J.-M. Caillol, D. Levesque, and J.-J. Weis, *J. Chem. Phys.* **116**, 10794 (2002).
 [41] E. Luijten, M. E. Fisher, and A. Z. Panagiotopoulos, *J. Chem. Phys.* **114**, 5468 (2001).
 [42] E. Luijten, M. E. Fisher, and A. Z. Panagiotopoulos, *Phys. Rev. Lett.* **88**, 185701 (2002).
 [43] G. H. Fredrickson and E. Helfand, *J. Chem. Phys.* **87**, 67 (1987).
 [44] V. E. Podneks and I. W. Hamley, *Pis'ma Zh. Eksp. Teor. Fiz.* **64**, 564 (1996).
 [45] Y. Levin, C. J. Mundy, and K. A. Dawson, *Phys. Rev. A* **45**, 7309 (1992).
 [46] A. Ciach, W. T. Gózdź, and G. Stell, *J. Phys.: Condens. Matter* **18**, 1629 (2006).
 [47] N. V. Brilliantov, C. Bagnuls, and C. Bervillier, *Phys. Lett. A* **245**, 247 (1998).
 [48] D. J. Amit, *Field Theory, the Renormalization Group and Critical Phenomena* (World Scientific, Singapore, 1984).
 [49] J. Zinn-Justin, *Quantum Field Theory and Critical Phenomena* (Clarendon, Oxford, 1989).